Supplement of Atmos. Chem. Phys., 24, 1361–1388, 2024
https://doi.org/10.5194/acp-24-1361-2024-supplement

Atmospheric Chemistry and Physics
Open Access
EGU

Supplement of

Diurnal variations in oxygen and nitrogen isotopes of atmospheric nitrogen dioxide and nitrate: implications for tracing NO_x oxidation pathways and emission sources

Sarah Albertin et al.

Correspondence to: Sarah Albertin (sarah.albertin@univ-grenoble-alpes.fr)

S1. NO_2 photolysis rate

The NO_2 photolysis rate (J_{NO_2}) was calculated for the sampling periods using a boxmodel (CiTTyCAT version 2.02; Pugh et al., 2012) with the Fast-J photolysis scheme of Wild et al. (2000). The surface albedo (SA) was fixed to 0.65 which is between fresh-snow and old-snow albedo (Gardner and Sharp, 2010). Calculated J_{NO_2} was not constrained with cloud coverage which could induce overestimations. Based on visual observations, weather conditions during the two sampling periods (SP 1 and SP 2) were very stable with no cloud cover, whereas clouds were observed from February 22 to 23. To assess cloud cover and its effect on J_{NO_2} more quantitatively, we used direct shortwave radiation data (Dir_SWdown in W m^{-2}) from the S2M (SAFRAN–SURFEX/ISBA–Crocus–MEPRA; Vernay et al., 2022) reanalysis (open access dataset at https://doi.org/ 10.25326/37#v2020.2). Figure S1 shows the sensitivity of Dir_SWdown to the presence of clouds from February 22 to 23 while on February 20, 21, 24 and 25 Dir_SWdown values are higher and reproducible. This comparison confirms the representativeness of J_{NO_2} values calculated during SP1 and SP2 with respect to meteorological conditions.

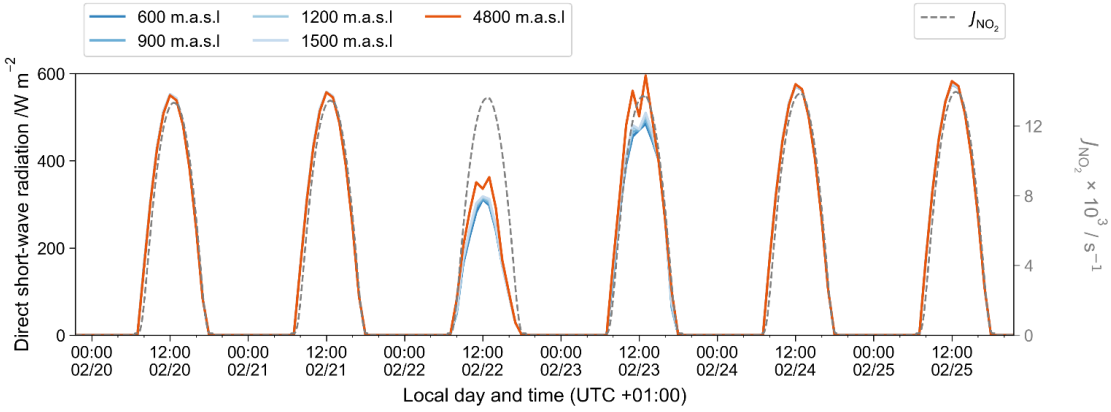

Figure S1. Temporal evolution of the direct short wave radiation (solid colored line) from the S2M (SAFRAN–SURFEX/ISBA–Crocus–MEPRA; Vernay et al., 2022) reanalysis at five altitudes from February 20th to February 25th in 2021 and of the NO_2 photolysis rate (J_{NO_2}, dashed grey line) from CiTTyCAT boxmodel output.

S2. Atmospheric NO_2 isotopic data

Sampling interval (start – end)	Mean NO_2 /nmol mol^{-1}	$\delta^{18}O(NO_2)$ /‰	$\Delta^{17}O(NO_2)$ /‰	$\delta^{15}N(NO_2)$ /‰
19/02 21:00 – 20/02 00:30	19.5 ± 2.0	57.4 ± 0.9	20.2 ± 0.3	–6.4 ± 0.3
20/02 00:30 – 20/02 04:30	13.7 ± 1.8	54.9 ± 0.9	19.9 ± 0.3	–9.0 ± 0.3
20/02 04:30 – 20/02 07:30	23.2 ± 7.7	56.9 ± 0.9	19.9 ± 0.3	–3.9 ± 0.3
20/02 07:30 – 20/02 10:30	38.1 ± 6.6	86.9 ± 0.9	29.4 ± 0.3	7.2 ± 0.3
20/02 10:30 – 20/02 13:30	29.1 ± 15.1	109.7 ± 0.9	37.3 ± 0.3	12.3 ± 0.3
20/02 13:30 – 20/02 16:30	14.0 ± 13.0	112.3 ± 0.9	40.8 ± 0.3	–0.7 ± 0.3
20/02 16:30 – 20/02 18:00	50.1 ± 16.2	75.0 ± 0.9	23.3 ± 0.3	7.0 ± 0.3
20/02 18:00 – 20/02 21:00	35.4 ± 10.3	61.8 ± 0.9	22.1 ± 0.3	–3.6 ± 0.3
24/02 07:30 – 24/02 10:30	41.7 ± 10.6	75.4 ± 0.9	22.3 ± 0.3	19.7 ± 0.3
24/02 10:30 – 24/02 13:30	23.3 ± 21.9	105.5 ± 0.9	35.0 ± 0.3	16.5 ± 0.3
24/02 13:30 – 24/02 16:30	4.5 ± 1.8	88.3 ± 8.8*	34.4 ± 3.4*	–5.4 ± 0.3
24/02 16:30 – 24/02 18:00	16.5 ± 9.6	61.7 ± 0.9	20.9 ± 0.3	1.2 ± 0.3
24/02 18:00 – 24/02 21:00	33.6 ± 3.5	63.1 ± 0.9	21.6 ± 0.3	–0.1 ± 0.3
24/02 21:00 – 25/02 00:00	14.7 ± 8.2	57.3 ± 0.9	20.0 ± 0.3	–5.2 ± 0.3
25/02 00:00 – 25/02 04:00	8.1 ± 1.2	52.8 ± 0.9	19.6 ± 0.3	–10.0 ± 0.3
25/02 04:00 – 25/02 07:30	17.6 ± 15.5	55.8 ± 0.9	20.1 ± 0.3	–1.5 ± 0.3

Table S1. Summary table of: atmospheric NO_2 sampling periods, ambient NO_2 mixing ratio (mean ± standard deviation over the sampling period) and measurement of $\delta^{18}O$, $\Delta^{17}O$, and $\delta^{15}N$ in NO_2. *Sample corrected from a blank of 14.0 % with an uncertainty of 10 % and assuming a blank $\Delta^{17}O$ at 0 ‰. Start and end datetimes (local time, UTC +01:00) represent when the denuder sample started and ended to be collected, respectively. All data represent the mean value over each sampling period. Uncertainty of $\Delta^{17}O$ and $\delta^{15}N$ data represents the accuracy of the analytical method (estimated as the standard deviation of the residuals between measurements of the reference materials and their expected values).

S3. Atmospheric nitrate isotopic data

Sampling interval (start – end)	NO_3^- /μg m^{-3}	$\delta^{18}O(NO_3^-)$ /‰	$\Delta^{17}O(NO_3^-)$ /‰	$\delta^{15}N(NO_3^-)$ /‰
19/02 21:00 – 20/02 00:30	2.0	55.1 ± 4.5	20.9 ± 0.4	1.6 ± 0.2
20/02 00:30 – 20/02 07:30	0.5	56.1 ± 4.4	21.0 ± 1.1	–0.3 ± 0.2
20/02 07:30 – 20/02 10:30	1.4	54.6 ± 3.8	18.3 ± 0.5	12.0 ± 0.1
20/02 10:30 – 20/02 13:30	1.1	62.5 ± 3.6	21.5 ± 0.1	14.9 ± 0.1
20/02 13:30 – 20/02 16:30	0.4	67.2 ± 2.2	26.1 ± 0.4	–1.3 ± 0.2
20/02 16:30 – 20/02 18:00	0.3	56.9 ± 4.2	20.9 ± 0.9	1.9 ± 0.3
20/02 18:00 – 20/02 21:00	0.6	53.1 ± 0.6	18.7 ± 0.2	2.5 ± 0.3
24/02 07:30 – 24/02 10:30	1.9	56.3 ± 1.1	18.6 ± 0.3	9.7 ± 0.1
24/02 10:30 – 24/02 13:30	3.4	67.5 ± 4.0	24.7 ± 0.6	5.5 ± 0.1
24/02 13:30 – 24/02 16:30	1.1	76.1 ± 2.6	28.1 ± 0.4	–3.8 ± 1.1
24/02 16:30 – 24/02 18:00	0.9	74.2 ± 1.2	27.2 ± 0.1	–4.2 ± 0.0
24/02 18:00 – 24/02 21:00	0.9	68.2 ± 2.3	24.5 ± 0.6	–1.4 ± 0.1
24/02 21:00 – 25/02 00:00	0.9	63.9 ± 1.3	22.2 ± 0.5	–0.5 ± 0.1
25/02 00:00 – 25/02 07:30	0.5	61.7 ± 3.0	22.8 ± 0.6	–1.5 ± 0.1

Table S2. Summary table of: atmospheric NO_3^- sampling periods, NO_3^- mass concentration determined by ion chromatography and isotopic measurements ($\delta^{18}O$, $\Delta^{17}O$, and $\delta^{15}N$). Start and end datetimes (local time, UTC +01:00) represent when the filter sample started and ended to be collected, respectively. All data represent the mean value over each sampling period. Uncertainty of isotopic data represents the standard deviation of the residuals between the sample measurement and the mean value of triplicates. Uncertainty of the analytical protocol averaged at ±0.4 ‰ and at ±0.3 ‰ for $\Delta^{17}O$ and $\delta^{15}N$, respectively.

S4. International isotopic reference materials

Salt	Standard name	$\delta^{17}O$ /‰	$\delta^{18}O$ /‰	$\Delta^{17}O$ /‰	$\delta^{15}N$ /‰
$NaNO_3$	USGS-35	51.5	57.5	21.6	2.7
$KNO_3/NaNO_3$	USGS 34/35, 50:50	16.5	12.5	10.9	0.3
KNO_3	USGS-34	–14.8	–27.9	–0.3	–1.8
KNO_3	USGS-32	13.4	25.7	0	180
KNO_2	RSIL-N7373		4.2		−79.6
KNO_2	RSIL-N10219		88.5		2.8
KNO_2	RSIL-N23		11.4		3.7

Table S3. International isotopic reference materials used to calibrate isotopic measurements of atmospheric NO_2 and NO_3^- samples.

S5. Ambient atmospheric observations in Chamonix

Sampling interval (start – end)	NO /nmol mol^{-1}	NO_2 / nmol mol^{-1}	O_3 / nmol mol^{-1}	PM_{10} /ug m^{-3}	$PM_{2.5}$ /ug m^{-3}
19/02 21:00 – 20/02 00:30	0.7 ± 0.3	19.5 ± 2.1	41 ± 1.5	28.7 ± 2.0	22.8 ± 2.0
20/02 00:30 – 20/02 04:30	0.2 ± 0.1	13.7 ± 1.8	7.2 ± 0.7	21.2 ± 6.9	17.4 ± 5.1
20/02 04:30 – 20/02 07:30	3.7 ± 4.1	23.3 ± 7.7	3.7 ± 2.1	9.0 ± 4.3	6.9 ± 3.9
20/02 07:30 – 20/02 10:30	32.8 ± 33.7	38.1 ± 6.7	1.7 ± 0.4	14.0 ± 9.3	10.9 ± 7.6
20/02 10:30 – 20/02 13:30	31.2 ± 35.6	29.2 ± 15.1	13.5 ± 11.9	24.7 ± 11.5	8.9 ± 8.1
20/02 13:30 – 20/02 16:30	5.6 ± 6.6	14.1 ± 13.1	28.8 ± 5.1	15.7 ± 9.3	3.6 ± 1.7
20/02 16:30 – 20/02 18:00	22.2 ± 6.5	50.2 ± 16.3	13.7 ± 7.7	39.8 ± 10.2	8.7 ± 2.5
20/02 18:00 – 20/02 21:00	4.9 ± 5.3	35.4 ± 10.4	2.9 ± 1.3	20.1 ± 2.8	13.8 ± 2.0
24/02 07:30 – 24/02 10:30	113.6 ± 53.5	41.8 ± 10.6	0.5 ± 0.4	46.9 ± 5.8	31.3 ± 3.9
24/02 10:30 – 24/02 13:30	47.4 ± 70.4	23.4 ± 22.0	13.9 ± 13.2	90.9 ± 34.6	33.5 ± 3.8
24/02 13:30 – 24/02 16:30	1.3 ± 0.4	4.6 ± 1.8	29.9 ± 0.8	114.5 ± 2.1	37.6 ± 0.5
24/02 16:30 – 24/02 18:00	4.8 ± 3.6	16.5 ± 9.7	23.5 ± 6.2	127.0 ± 11.5	38.5 ± 0.9
24/02 18:00 – 24/02 21:00	8.2 ± 6.4	33.6 ± 3.5	1.8 ± 1.2	53.7 ± 17.8	31.9 ± 5.4
24/02 21:00 – 25/02 00:00	1.1 ± 1.4	14.8 ± 8.2	3.1 ± 2.7	53.4 ± 147	35.7 ± 9.9
25/02 00:00 – 25/02 04:00	0.1 ± 0.1	8.1 ± 1.3	10.6 ± 3.7	31.0 ± 11.5	20.7 ± 7.7
25/02 04:00 – 25/02 07:30	6.2 ± 15.0	17.6 ± 15.6	11.5 ± 5.6	17.9 ± 2.2	12.0 ± 1.4

Table S4. Summary of ambient atmospheric observations in Chamonix averaged over each denuder sampling period (mean value ± the standard deviation over the sampling period). Start and end datetimes (local time, UTC+01:00) represent when the denuder sample started and ended to be collected, respectively. Surface NO_x mixing ratios were measured at the sampling site using an incoherent broadband cavity-enhanced absorption spectrometer for NO_2 (IBBCEAS; Barbero et al., 2020) and an optical-feedback cavity-enhanced absorption spectrometer for NO (OFCEAS; Richard et al., 2018). O_3 mixing ratio was monitored at the local air quality monitoring site located a kilometre north of the sampling site (Environnement SA®, O3 42M; https://www.atmo-auvergnerhonealpes.fr/, last access: 5 November 2021). Particulate matter (PM_{10}, $PM_{2.5}$) concentrations were monitored by an optical particle counter (GRIMM®, EDM 164).

S6. Temperature, kinetic and isotopic equilibrium constants

Sampling interval (start – end)	$T_{surface}$ /K	k_{NO+O_3} $\times 10^{-14}$ /cm^{-3} mol^{-1} s^{-1}	$\alpha_{EIE(NO_2/NO)}$	$\alpha_{KIE(NO+O_3)}$
19/02 21:00 – 20/02 00:30	274.6	1.14	1.045	0.994
20/02 00:30 – 20/02 04:30	272.7	1.10	1.046	0.994
20/02 04:30 – 20/02 07:30	271.6	1.08	1.046	0.994
20/02 07:30 – 20/02 10:30	271.0	1.07	1.046	0.994
20/02 10:30 – 20/02 13:30	274.6	1.12	1.045	0.994
20/02 13:30 – 20/02 16:30	287.5	1.40	1.042	0.994
20/02 16:30 – 20/02 18:00	288.3	1.44	1.042	0.994
20/02 18:00 – 20/02 21:00	280.3	1.27	1.044	0.994
24/02 07:30 – 24/02 10:30	274.0	1.12	1.045	0.994
24/02 10:30 – 24/02 13:30	279.4	1.22	1.044	0.994
24/02 13:30 – 24/02 16:30	289.3	1.45	1.041	0.994
24/02 16:30 – 24/02 18:00	289.2	1.45	1.042	0.994
24/02 18:00 – 24/02 21:00	284.2	1.35	1.043	0.994
24/02 21:00 – 25/02 00:00	278.3	1.22	1.044	0.994
25/02 00:00 – 25/02 04:00	277.1	1.19	1.044	0.994
25/02 04:00 – 25/02 07:30	276.2	1.17	1.045	0.994

Table S5. Summary table of measured surface temperature, calculated k_{NO+O_3}, $\alpha_{EIE(NO_2/NO)}$ and $\alpha_{KIE(NO+O_3)}$.

S7. Temperature profiles

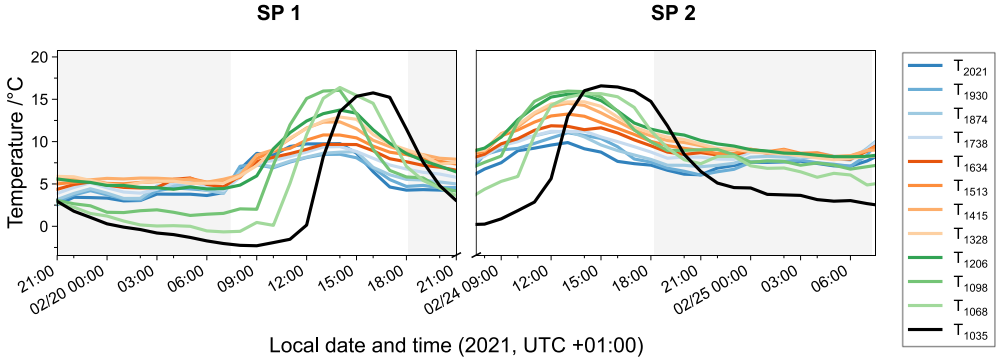

Figure S2. Temporal evolution of air temperature during the two sampling periods (February 19th–20th and February 24th–25th). The profiles are plotted using observations of 13 portable temperature loggers placed at two ground−based stations in Chamonix at 1035 m.a.s.l and at 1068 m.a.s.l and fixed along the Plan−Praz cable car (45°55′21.53″ N, 6°52′11.68″ E) from 1098 m.a.s.l to 2021 m.a.s.l.

S8. Atmospheric observations in Chamonix in February 2021

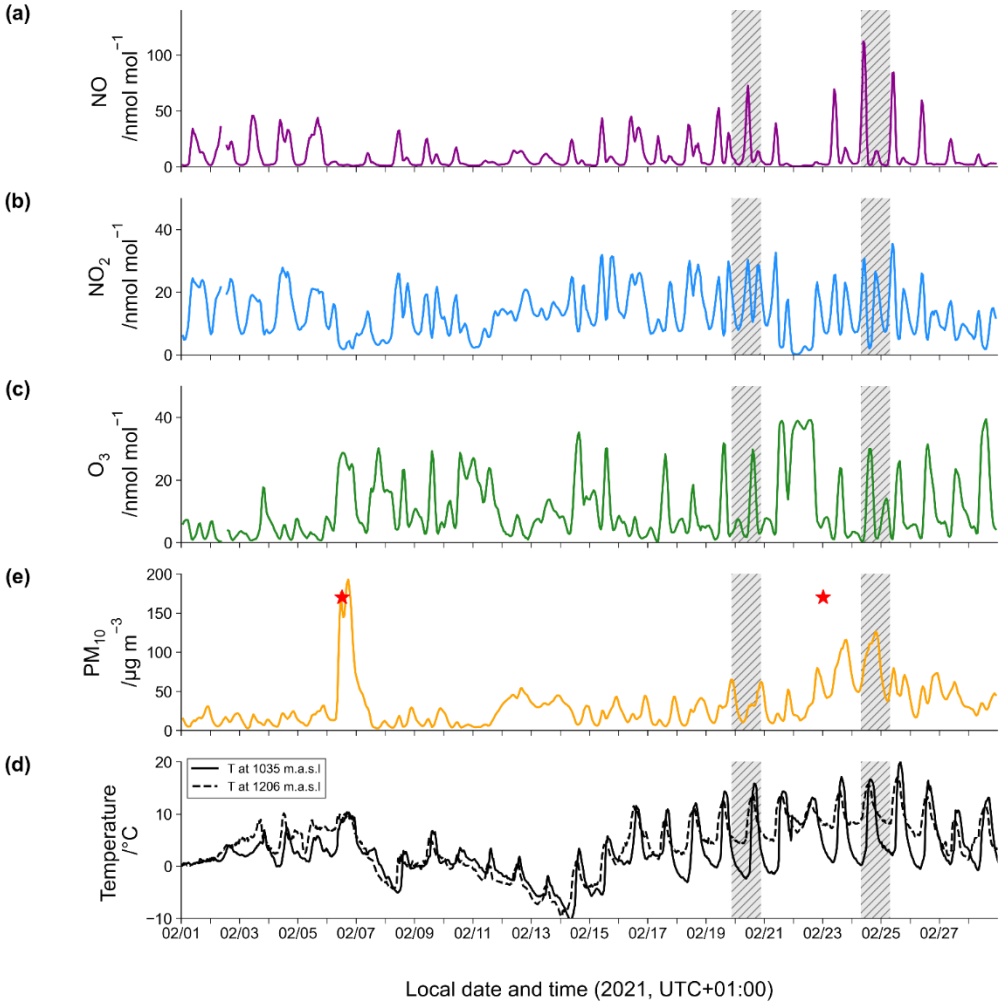

Figure S3. Temporal evolution in February 2021 in Chamonix of the hourly mean of **(a)** NO mixing ratio (purple line), **(b)** NO_2 mixing ratio (blue line), **(c)** O_3 mixing ratio (green line), **(d)** PM_{10} mass concentration (orange line) and **(e)** temperature at the surface (black line) and at 1206 m.a.s.l (dashed black line). Saharan dust events that occurred in February 2021 are represented by the red stars. Grey shaded areas represent sampling periods for this study. Data provided by the air quality monitoring site (https://www.atmo-auvergnerhonealpes.fr/, last access: 5 November 2021).

S9. Evidences of a Saharan dust event in Chamonix on February 24-25 2021

The NASA AQUA satellite images from MODIS show the formation of a dusty air mass above the Saharan region on 20 February and the displacement of this air mass in the following days to the south of France (Figure

S4). In addition, backtracking trajectory (HYSPLIT) allows to visualise the entrance in the Chamonix valley of air masses coming from the south on 24 February (Figure S3).

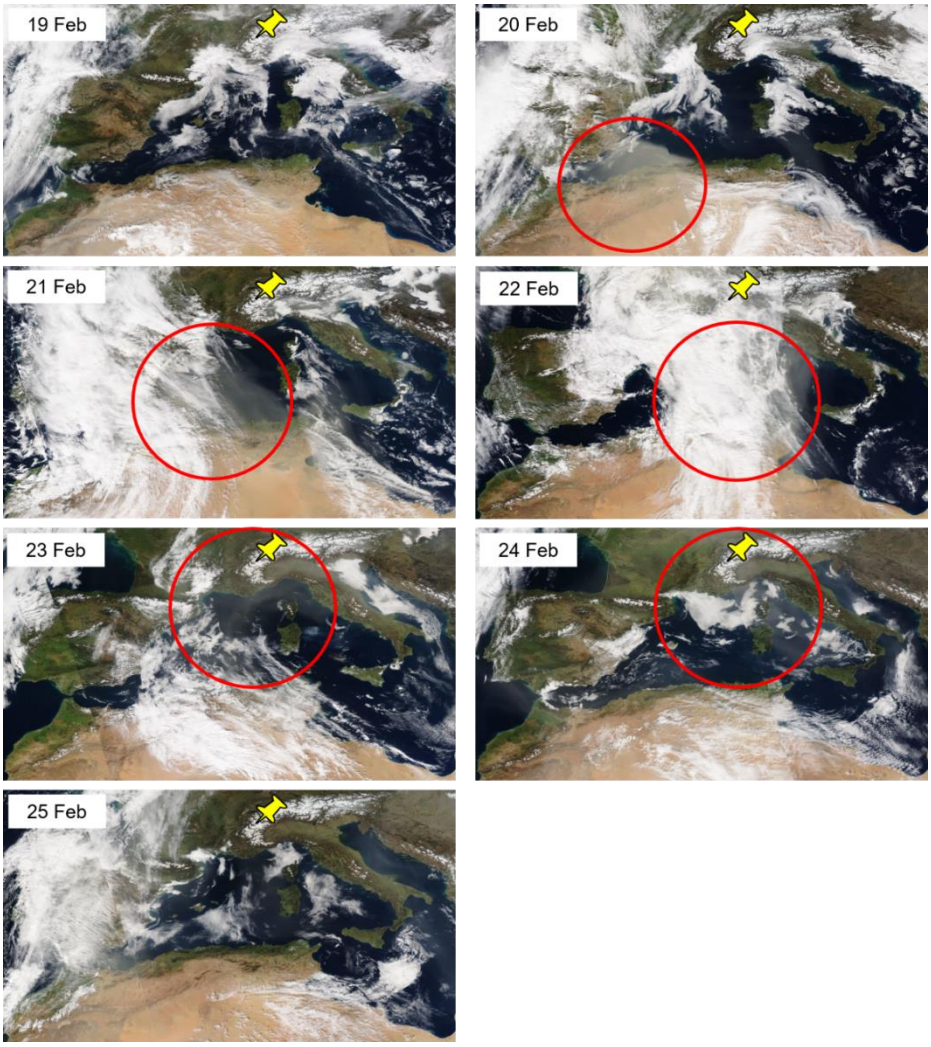

Figure S4. Images from the AQUA satellite (MODIS; © NASA) from 19 February 2021 to 25 February 2021. One can see a plume of Saharan dust forming over North Africa on 20 February (localised by the red circle) and moving above the south of France and the Alps until 24 February. The yellow pin points to Chamonix, France.

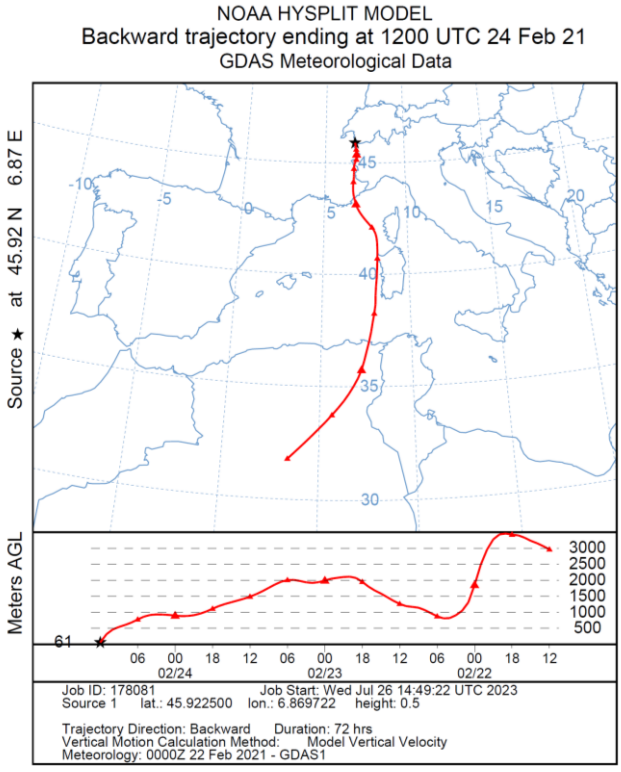

Figure S5. HYSPLIT 72 hours backward trajectory on 24 February 2021 ending at Chamonix, France, at 12:00 UTC (13:00 local time). The model was run every 6 hours. The starting height (in meter above ground level) is half of the boundary layer height estimated by the model from meteorological data set.